Plain Geopolymer Concrete Cross-Section Surface Analysis After Creep and Shrinkage Tests in Compression and Tension

Rihards Gailitis, Andina Sprince, Leonids Pakrastins, Kinga Korniejenko, and Tomass Kozlovskis

Abstract Low calcium alkali-activated cement composite known as geopolymer has been around for more than 40 years. The main benefit of geopolymer based composites is the environmental aspect—it is partially made by utilizing waste products, such as fly-ash, slags, and others. It has been estimated that geopolymer binder production makes up to 6 times less CO_2 than the production of Portland cement. Due to the polymerization or in other words nature of the geopolymer binding process, there are some differences in creep and shrinkage development. Because of this microstructure of the specimen could be dissimilar to ordinary Portland cement. There has been an absence of investigations regarding the geopolymer composite long-term properties and micro-analysis. Also, the conditions affecting the long-term properties of the geopolymer composites have been little studied. The subject of the research is geopolymer concrete that has been tested for creep and shrinkage in compression and tension. The specimens for microstructure analysis were acquired from the cylindrical shape (compression) and compact tension (tension) specimens. Polished sections were used for SEM microanalysis. Acquired polished section image cross-sections were analyzed by determining the amount of geopolymer binder, filler, and air void in the analyzed cross-section. The results were cross-referenced with creep and shrinkage test results. After creep and shrinkage tests in compression and tension specimen cross-section zones that have been subjected to the highest stresses were chosen and analyzed. The article's main aim is to determine the geopolymer composite microstructure and applied load influence on long-term properties.

Keywords Geopolymer concrete · Polished section microanalysis · Long-term properties · Compression · Tension

R. Gailitis (✉) · A. Sprince · L. Pakrastins · T. Kozlovskis
Riga Technical University, Riga, Latvia
e-mail: rihards.gailitis@edu.rtu.lv

K. Korniejenko
Cracow University of Technology, Cracow, Poland

F. Kanavaris et al. (eds.), *International RILEM Conference on Early-Age and Long-Term Cracking in RC Structures*, RILEM Bookseries 31,
https://doi.org/10.1007/978-3-030-72921-9_2

1 Introduction

Alkali activated cement composites based on industrial waste products such as fly ash, blast furnace slag, etc., have been considered a cement for the future [1, 2]. As the cement consumption, year by year, go up and now is responsible for 1.5 billion tonnes of CO_2 emissions annually. It becomes a significant issue around 36% of global energy consumption to research viable alternatives for less polluting binder usage with comparable properties regarding workability [3]. The use of alkali-activated materials is beneficial to CO_2 reduction. It is positive from a sustainable environment standpoint as it incorporates such industrial by-products as fly ash and slag [4]. The issue regarding wide usage of geopolymer is mainly due to the binder hardening or the polymerization process. This process requires heat; the temperature can vary from 40 to 100 °C (depending on fly ash or slag type and alkali activator) and the polymerization time from 12 to 48 h and more, therefore, excluding on-site construction works due to difficulties in achieving satisfactory structural performance [5].

Geopolymer is a low calcium alkali-activated cement composite. It is formed due to a silicon and aluminium reaction activated by hydroxide silicates from sodium and potassium alkali activating solution [6, 7].

Geopolymer concrete has similar compressive strength to regular Portland cement (PC) based composites. Unlike regular PC, geopolymer composites 85% of their final compressive strength can reach in 48 h [8]. Long-term property wise geopolymer composites have 78% less shrinkage and 50% less creep strains than foamed regular concrete and a bit worse than regular PC composites [9].

Creep and shrinkage are well-known phenomena for cement and cement-like based composite materials, and it may influence the lifetime of structures. Most of the creep and shrinkage effects develop in the first ten years after construction. It is expected that the creep and shrinkage development after the first ten years are not significant and have a small impact on the performance of the structure [10–12]. Concrete and similar materials are considered to insufficient strain capacity and low tensile strength. And, consequently, they are brittle and susceptible to cracking. For cementitious composites under compression damages first happen in the paste-aggregate interface. The tensile stresses are necessary to determine long-term tensile properties for these materials [13]. Furthermore, because of the difficulties of performing tensile creep tests and differences in creep mechanisms in tension and compression, it is equally important to determine the factors that influence creep properties in compression and tension [14].

The paper focuses on the microstructure differences in specimens that have been used in creep tests in compression, tension, and shrinkage tests. Therefore, microstructure images were acquired and analysed. Results of image analysis were cross-referenced with the creep and shrinkage curves to determine whether there are notable correlations.

2 Materials and Methods

2.1 Geopolymer Mix Preparation

Geopolymer specimen matrixes were based on fly ash sourced from the power plant based in Skawina city (Poland). The fly ash contains spherical aluminosilicate particles and contains oxides such as SiO_2 (47.81%), Al_2O_3 (22.80%). The high value of SiO_2 and Al_2O_3 allows polymerization [15].

Geopolymer specimens were prepared using sodium promoter, fly ash, and sand (sand and fly ash ratio—1:1). The geopolymer activation process has been made by 10M NaOH solution and the sodium silicate solution (at a rate of 1:2.5). The technical NaOH in flake form and tap water with sodium silicate R–145 solution is used to make the composite solution. The alkaline solution was prepared by pouring sodium silicate and water over solid sodium hydroxide into sodium silicate and water aqueous solution. The solution was mixed, and the temperature was stabilized. The fly ash, sand, and alkaline solution were mixed for about 15 min using a low-speed mixing machine (to achieve homogenous paste). Then the geopolymers were poured into the plastic moulds, as is shown in Fig. 1. The specimens were hand-formed, and then the air bubbles were removed by vibrating the mass. Moulds were heated in the laboratory dryer for 24h at 75 °C. Then, the specimens were unmolded. All the geopolymer specimen preparation was done at Cracow University of Technology (CUT), Poland.

(a) (b) (c)

Fig. 1 Geopolymer composite preparation (**a**) and moulding process (**b** and **c**), CUT lab

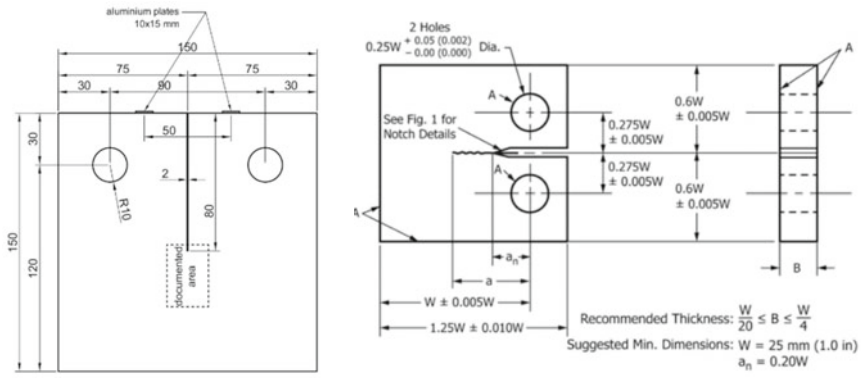

(a) (b)

Fig. 2 Geometry of the Compact Tension (CT) specimen [17, 18]

2.2 Test Specimen Preparation

For creep testing in compression, specimens were prepared according to RILEM TC 107-CSP recommendations [16]. All of the specimens were Ø 46 × 190 mm or approximately 1:4 diameter to height ratio. For the dial gauge attaching six aluminium plates were glued on specimens intended for creep testing in compression. Afterward, dial gauges were attached to those plates. For shrinkage specimens one aluminium plate was glued at the bottom and top part of each specimen. After that, shrinkage specimens were placed in a stand for shrinkage measurements.

For creep measuring in tension, compact tension (CT) shaped specimens were used [17]. Specimens were cut out from a cube that was 150 × 150 × 150mm. Each cut CT specimen was 15 mm thick. Afterward, the notch was cut as well as two bore holes were made (for attaching within a loading rig), as shown in Fig. 2.

The 2 mm wide notch in the CT specimen was sawn using a Proxxon MICRO MBS 240/E bandsaw. According to Fig. 2a, the aluminium plates were glued to specimens intended for creep and shrinkage tests. Plates were glued 25 mm to each side from the notch center. There were prepared 12 cylinders and 12 CT specimens.

2.3 Experimental Setup

When the specimens' preparation was done, compressive strength and tensile strength ultimate values were determined. The procedure is shown in Fig. 3.

The ultimate compressive load was determined using Controls Mod. Nr C56G2 press with a speed of 0.8 MPa/sec. The ultimate tensile load was determined using INSTRON 3000 All-Electric Dynamic Test Instrument with speed 0.15mm/sec.

(a) (b)

Fig. 3 Compressive (**a**) and tensile (**b**) strength determination, RTU lab

Determined strength values were compiled in Table 2. Following strengths determination, creep specimens were placed into lever test stands and were loaded with a constant static load equal to 20% of the ultimate load values (see Fig. 4). With these stands, it is possible to apply constant loading to the specimens and to keep it uniform over a long period. Strains were measured using mechanical dial gauges "*И*Ч" with a scale interval of 1/100 mm and maximum measuring range of 10 mm.

To determine basic creep behavior, similarly shaped shrinkage specimens were placed in equivalent environmental conditions, and their strain changes were monitored (no load applied to the shrinkage specimens). Conclusions were made based on subtracting shrinkage strain values from the creep values. Figure 5 shows the test setups for shrinkage tests. All specimens were kept in a dry atmosphere of controlled relative humidity in standard conditions: temperature 20 ± 1 °C and relative humidity 48 ± 3%. The geopolymer specimen preparation and strength, long-term tests were done at Riga Technical University (RTU), Latvia.

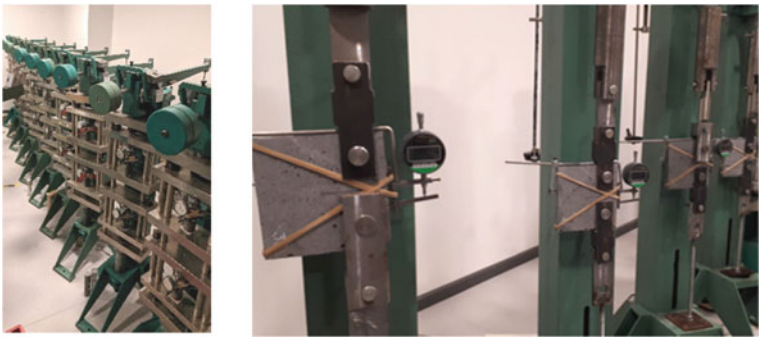

(a) (b)

Fig. 4 Creep specimen placement into compression (**a**) and tension (**b**) test stands, RTU lab

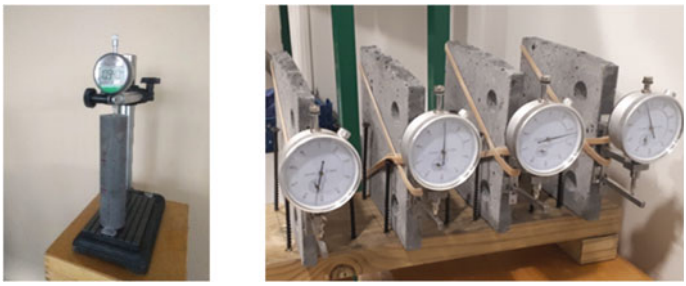

(a) (b)

Fig. 5 Shrinkage test setup for compression (**a**) and tension (**b**) specimens, RTU lab

2.4 Microstructure Composition Specimen Preparation

After all long-term tests, specimen cross-section parts for the scanning electron microscope (SEM) were prepared for microstructure composition determination. Figure 6 shows prepared compression and tension specimen samples for microstructure analysis.

For the specimens that have been subjected to compression tests, cylinders middle parts were cut into disc shape samples with a thickness of 15mm. Compact tension specimens (CT) middle part where notch ends were drilled. The drilled samples were with Ø 48 and 15 mm thickness. Afterward, all samples were polished according to the sequence described in Table 1.

When the microanalysis samples were prepared, they were delivered to Cracow University of Technology (CUT) and covered with gold. For each sample, the characteristic cross-section areas were chosen and marked. The characteristic cross-section areas were analyzed. These sample areas were shown in Fig. 7.

(a) (b) (c)

Fig. 6 SEM samples preparation (**a**) SEM samples polishing (**b**) and prepared samples before the gold plating (**c**), RTU lab

Table 1 Specimen surface polishing sequence

Polishing stage number	Polishing compound (sandpaper or paste grade) type	Polishing cycle time, minutes	Compression force to specimen polishing surface, daN
1	P180	2	2.5
2	P320	2	2.5
3	P600	2	2.5
4	P1000	2	2.5
5	P1200	2	2.5
6	3 μm	4	2.5

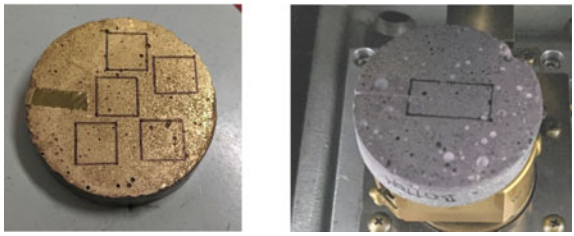

(a) (b)

Fig. 7 Compression (**a**) and tension (**b**) SEM samples, CTU lab

For specimens that have been subjected to compression testing, the cross-section was divided into five squared (10x10mm) section parts distributed into the central and peripheral part of the specimen cross-section. Still, for the specimens subjected to tensile loads (CT specimens), the microanalysis is done to the cross-section part near the notch and deeper into the specimen.

The SEM microanalysis was done in JEOL JSM-820. The achieved SEM images afterward were compiled together and divided into layers using Adobe Photoshop CC. The division into layers was based on partition type within cross-section (matrix, filler, air voids). For each of these partitions, the RGB tone was allocated. The process is shown in Fig. 8. The layer dividing process begins with filler layer separation that was continued with the void layer.

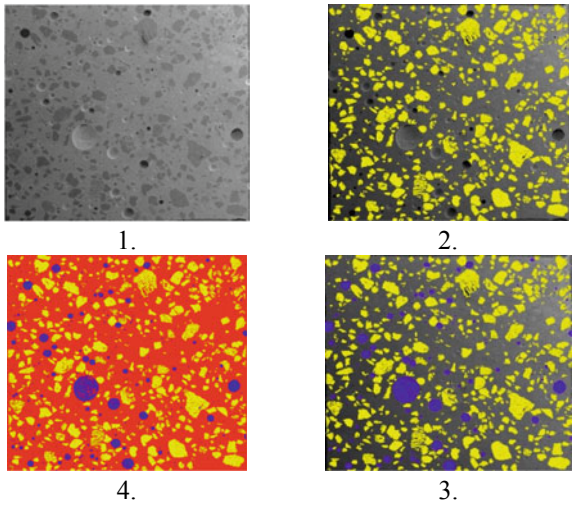

Fig. 8 Image dividing sequence in layers and tone allocation

When the image dividing and RGB tone allocation was done, the specific tone image pixels were counted and registered. By doing so, the composition amount of the studied cross-section was acquired.

3 Results and Discussion

The compressive and tensile strength of the tested specimens is compiled in Table 2. Specimens intended for creep tests were subjected to a load equal to 20% of the load values shown in Table 2.

After the compression and tension ultimate load tests, the creep and shrinkage tests were carried out for 91 days (more than three months). Tests were started on the 7th day since the preparation of the specimens. The creep and shrinkage curves for compression and tension specimens are shown in Fig. 9.

The curves in Fig. 9a and b show that throughout testing time creep strains for CT specimens are almost half of the creep strains in compression. The difference on average is 46%. It is also apparent that the amount of elastic strain at the beginning

Table 2 Compressive and tensile ultimate load values

Specimen type	Ultimate load value, average (kN)	Average compressive and tensile strength, MPa
Cylinders, plain geopolymer	60.35	61.44
CT, plain geopolymer	0.28	5.13

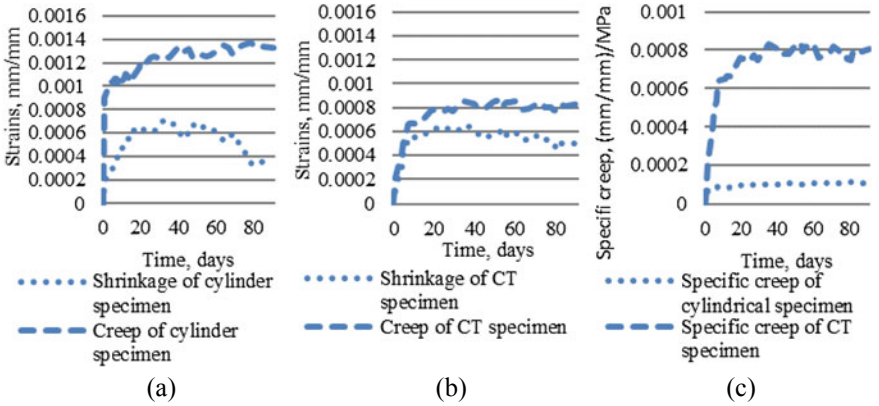

Fig. 9 Creep and shrinkage curves of compression (**a**) and tension (**b**) specimens and specific creep (**c**) of compression and tension specimens

of the tests and further strain development characteristics are different for specimens in compression and tension. Furthermore, specific creep in tension (Fig. 9c) is more than 7 times greater that in compression. It leads to a conclusion that there are significant microstructural differences to the microstructural development of the specimens tested in compression and tension, and also, plain geopolymer composite has similar creep properties as the regular Portland cement-based composites. Also, the shrinkage curve for CT specimens in Fig. 9b clearly shows that specimens have properly polymerized and achieved their modulus of elasticity close to what could be considered as the final modulus of elasticity value. Therefore, the notch is opening, unlike Portland cement composites that due to hydration would close the notch.

The obtained cross-section composition results are shown in Table 3.

First of all, it becomes apparent that the cylinder's air void wise was much better shape than the cube used to make CT specimens. The all in all cross-section composition analysis show that porosity for CT shaped specimens on average is from 24% to 32% higher than cylinder-shaped specimens. It means that due to the cube's dimension, it is much harder for air to escape from the middle parts of the cube while it was vibrated than it is for the air in the cylinder-shaped specimens.

Table 3 Compressive and tensile ultimate load values

Test type	Specimen type	Matrix amount in cross-section, %	Filler amount in cross-section, %	Air void amount in cross-section, %
Shrinkage	Cylinder	73.48	20.08	6.44
	CT	73.61	16.94	9.45
Creep	Cylinder	73.76	19.62	6.62
	CT	75.64	15.60	8.76

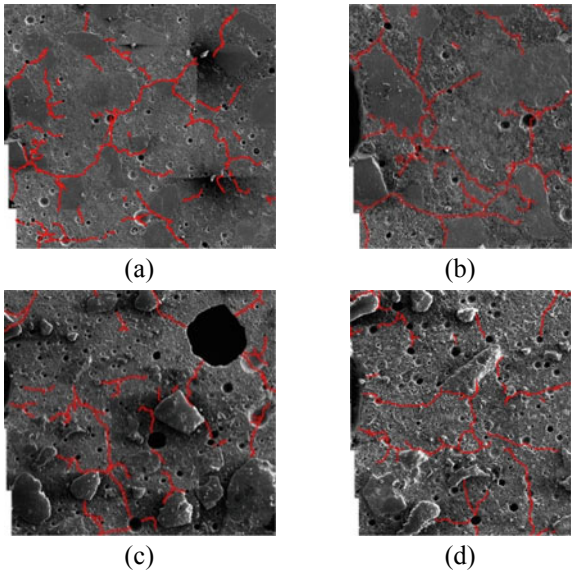

Fig. 10 Crack assessment of shrinkage specimen notch base at 100 times (**a**) and 200 times (**b**) magnification and creep specimen notch base at 100 times (**c**) and 200 times (**d**) magnification

The notch cross-section part's analysis was done to further determine the low amount of elastic strains for CT specimens.

In Fig. 10, the notch part (tip) is in the middle of the left-hand side of each image. Here it is apparent that there are a significant number of cacks in the notch area. Furthermore, the crack amount for creep specimens is close to shrinkage specimens with a slight increase to creep specimens. All that leads to thinking that due to early age testing, shrinkage plays a considerable role in the crack development, making specimens undergo larger plastic strains.

To further analyze the load impact to CT specimen cross-section notch zone (3mm from the beginning of the notch) was measured. The notch's overall general area and the notch's length and width from six equally spaced measurements along the notch length. The results are shown in Table 4.

It is clear to see that creep specimen notch basis was more deformed than shrinkage specimens. In the length of 3mm from the notch base, the notch area is average 5.7% bigger; thus, it was deformed than the notch part of the shrinkage specimens. Furthermore, while the width of the analyzed shrinkage specimens' notch part stays the same for the creep specimens, width increases on average by 0.168mm or 28.11%.

Table 4 Notch base part analysis

Test type	Average length of the notch, mm	Difference, %	Average width of the notch, mm	Difference, %	Average area of the notch, mm2	Difference, %
Shrinkage	2.979	1.2	0.684	5.4	1.974	5.7
Creep	3.016		0.723		2.094	

4 Conclusions

1. Compact tension (CT) specimens on average have a 5.15% higher amount of air voids than cylinder type specimens. The filler amount in the analyzed CT specimen cross-sections is 7.16% less than cylindrical specimen cross-sections, while the matrix amount stays the same. Therefore, while the cube specimens as a base of the CT specimen preparation for long-term tests are not bad, the CT specimen making directly in the right shape moulds would be considered a better practice for air void filler distribution wise.
2. The creep strain amount for the compression specimens is 35.8% higher than the creep strains for tension specimens. In contrast to ultimate load values, the difference is 99.54% in favor of the compression intended specimens.
3. Specific creep for specimens in compression is on average 85.92% less than for CT specimens. Therefore, geopolymer composites have 7.5 times larger creep strains in tension than in compression.
4. From the creep and shrinkage strain curves and notch base part cracks analysis, it is apparent that tension specimens, in this case, CT specimens, have lower elastic strain part and, in early stages, develop cracks in the base of the notch. Tension specimen elastic strains at the beginning of tests are on average 90.9% less than compression specimens.
5. Due to early age testing and lack of fiber reinforcement, the shrinkage strains play a considerable role in the crack development into the CT specimens and, therefore, the increased amount of plastic strains of the tension specimens. Tension specimens have 0.000379 mm/mm or 47.6% higher plastic strains than was determined by creep compression specimens.

Acknowledgements

1. This work has been supported by the European Regional Development Fund within the Activity 1.1.1.2 “Post-doctoral Research Aid” of the Specific Aid Objective 1.1.1 “To increase the research and innovative capacity of scientific institutions of Latvia and the ability to attract external financing, investing in human resources and infrastructure” of the Operational Programme “Growth and Employment” (No.1.1.1.2/VIAA/3/19/401). The authors acknowledge the support of the PROM programme no. PPI/PRO/2019/1/00013/U/001 which is co-financed by the European Social Fund under the Knowledge Education Development Operational Programme. This publication was supported by Riga Technical University’s Doctoral Grant programme.
2. The authors acknowledge the support of the PROM programme no. PPI/PRO/2019/1/00013/U/001 which is co-financed by the European Social Fund under the Knowledge Education Development Operational Programme.
3. This publication was supported by Riga Technical University’s Doctoral Grant programme.

References

1. Shi, C., Jiménez, A.F., Palomo, A.: New cements for the 21st century: the pursuit of an alternative to Portland cement. Cem. Concr. Res. **41**(7), 750–763 (2011)
2. Tu, W., Zhu, Y., Fang, G., Wang, X., Zhang, M.: Internal curing of alkali-activated fly ash-slag pastes using superabsorbent polymer. Cem. Concr. Res. **2019**(116), 179–190 (2018)
3. Kermeli, K., Edelenbosch, O.Y., Crijns-Graus, W., van Ruijven, B.J., Mima, S., van Vuuren, D.P., Worrell, E.: The scope for better industry representation in long-term energy models: modeling the cement industry. Appl. Energy **2019**(240), 964–985 (2018)
4. Rashad, A.M., Essa, G.M.F.: Effect of ceramic waste powder on alkali-activated slag pastes cured in hot weather after exposure to elevated temperature. Cement Concr. Compos. **2020**(111), 103617 (2019)
5. Kang, S.H., Jeong, Y., Kim, M.O., Moon, J.: Pozzolanic reaction on alkali-activated Class F fly ash for ambient condition curable structural materials. Construct. Build. Mater. **218**, 235–244 (2019)
6. Yan, S., He, P., Jia, D., Wang, J., Duan, X., Yang, Z., Wang, S., Zhou, Y.: Effects of high-temperature heat treatment on the microstructure and mechanical performance of hybrid C f -SiC f -(Al 2 O 3p) reinforced geopolymer composites. Compos. B: Eng. **114**, 289–298 (2017)
7. Linul, E., Korniejenko, K., ŞSerban, D.A., Negru, R., Marşavina, L., Łach, M., Mikuła, J.: Quasi-static mechanical characterization of lightweight fly ash-based geopolymer foams. In: IOP Conference Series: Materials Science and Engineering, vol. 416 (2018)
8. Assi, L.N., Carter, K., Deaver, E., Ziehl, P.: Review of availability of source materials for geopolymer/sustainable concrete. J. Cleaner Prod. **263**, 121–477 (2020)
9. Amran, M., Fediuk, R., Vatin, N., Lee, Y.H., Murali, G., Ozbakkaloglu, T., Klyuev, S., Alabduljabber, H.: Fibre-reinforced foamed concretes: a review. Materials **13**(19), 1–36 (2020)
10. Nastic, M., Bentz, E.C., Kwon, O., Papanikolaou, V., Tcherner, J.: Shrinkage and creep strains of concrete exposed to low relative humidity and high temperature environments. Nucl. Eng. Design **352**, 110–154 (2019)
11. Boumakis, I., Di Luzio, G., Marcon, M., Vorel, J., Wan-Wendner, R.: Discrete element framework for modeling tertiary creep of concrete in tension and compression. Eng. Fract. Mech. **200**, 263–282 (2018)
12. Rossi, P., Tailhan, J.L., Le Maou, F.: Comparison of concrete creep in tension and in compression: influence of concrete age at loading and drying conditions. Cement Concrete Res. **51**, 78–84 (2013)
13. Ranaivomanana, N., Multon, S., Turatsinze, A.: Basic creep of concrete under compression, tension and bending. Construct. Build. Mater. **38**, 173–180 (2013)
14. Cheng, Z.Q., Zhao, R., Yuan, Y., Li, F., Castel, A., Xu, T.: Ageing coefficient for early age tensile creep of blended slag and low calcium fly ash geopolymer concrete. Construct. Build. Mater. **262**, 119–855 (2020)
15. Korniejenko, K., Łach, M., Hebdowska-Krupa, M., Mikuła, J.: The mechanical properties of flax and hemp fibres reinforced geopolymer composites. IOP Conf. Series: Mater. Sci. Eng. **379**(1) (2018)
16. Acker, P., Agullo, L., Auperin, M., Carol, I., Carreira, D., Catarino, J., Chem, J.-C., Chiorino, M., Dougill, J., Huet, C., Kanstad, T., Kim, J.-K., Křístek, V., Republic, C., S Muller, H., Byung, G., Oh, H., Ožbolt, J., Reid, S., Wittmann, F.: RILEM TC 107-CSP: creep and shrinkage prediction models: principles of their formation. Recommendation Measurement of time-dependent strains of concrete. Mater. Struct. **31**, 507–512 (1998)
17. ASTM. E647—standard test method for measurement of fatigue crack growth rates. ASTM Book of Standards. 03(July), pp. 1–49 (2016)
18. Sprince, A., Pakrastinsh, L., Baskers, B., Gaile, L.: Crack development research in extra fine aggregate cement composites. Vide. Tehnologija. Resursi - Environment, Technology, Resources. **1**, 205–208 (2015)